

Supplement of Solid Earth, 9, 1299–1328, 2018  
<https://doi.org/10.5194/se-9-1299-2018-supplement>  
© Author(s) 2018. This work is distributed under  
the Creative Commons Attribution 4.0 License.



*Supplement of*

## **Failure criteria for porous dome rocks and lavas: a study of Mt. Unzen, Japan**

**Rebecca Coats et al.**

*Correspondence to:* Rebecca Coats ([r.coats@liverpool.ac.uk](mailto:r.coats@liverpool.ac.uk))

The copyright of individual parts of the supplement might differ from the CC BY 4.0 License.

Supplementary Figures

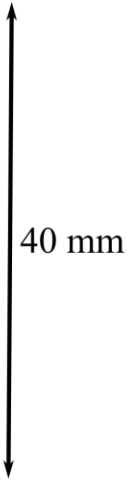
UNZ-1



UNZ-2



UNZ-4



40 mm

UNZ-5



UNZ-7



UNZ-8



UNZ-11



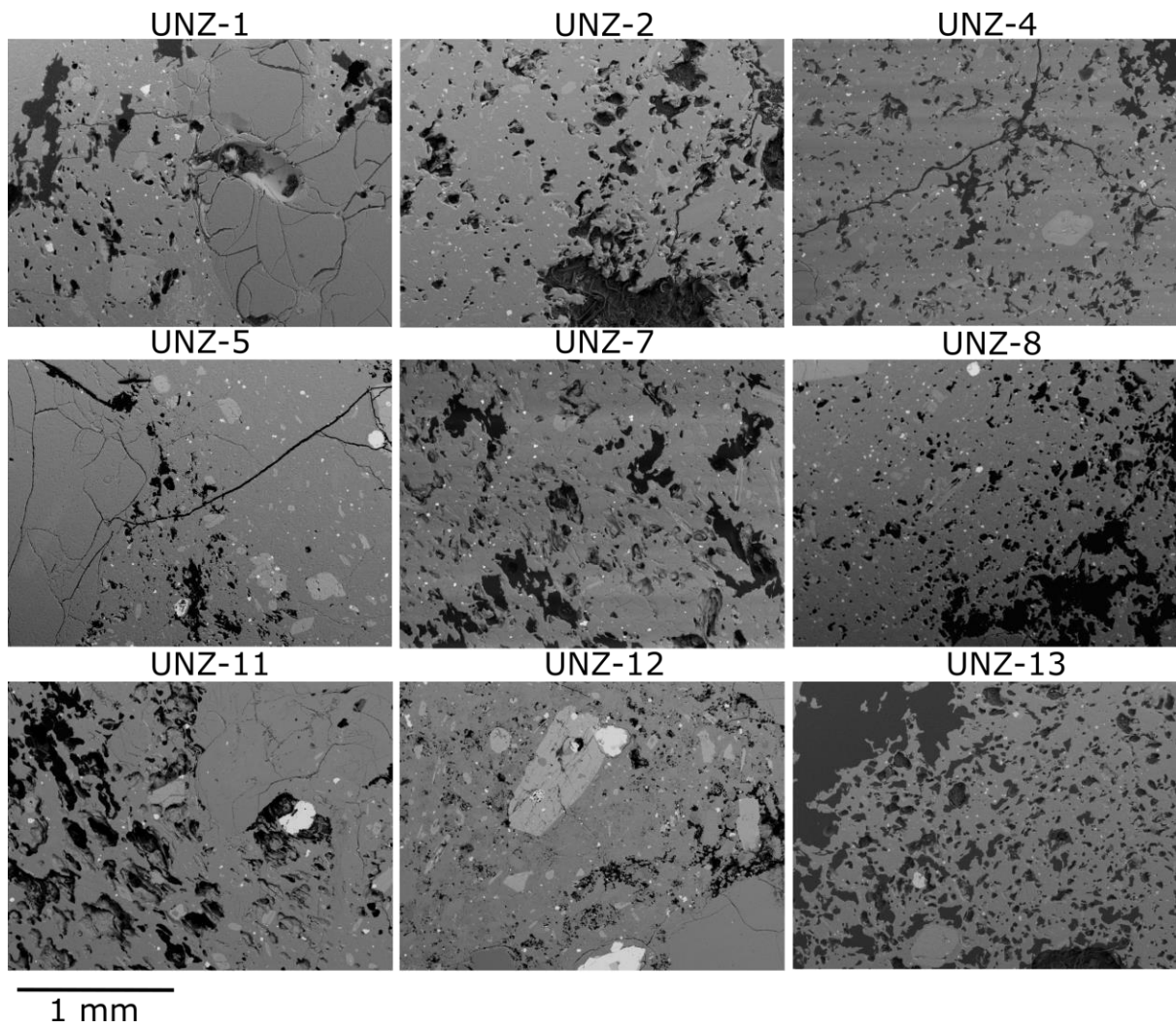
UNZ-12



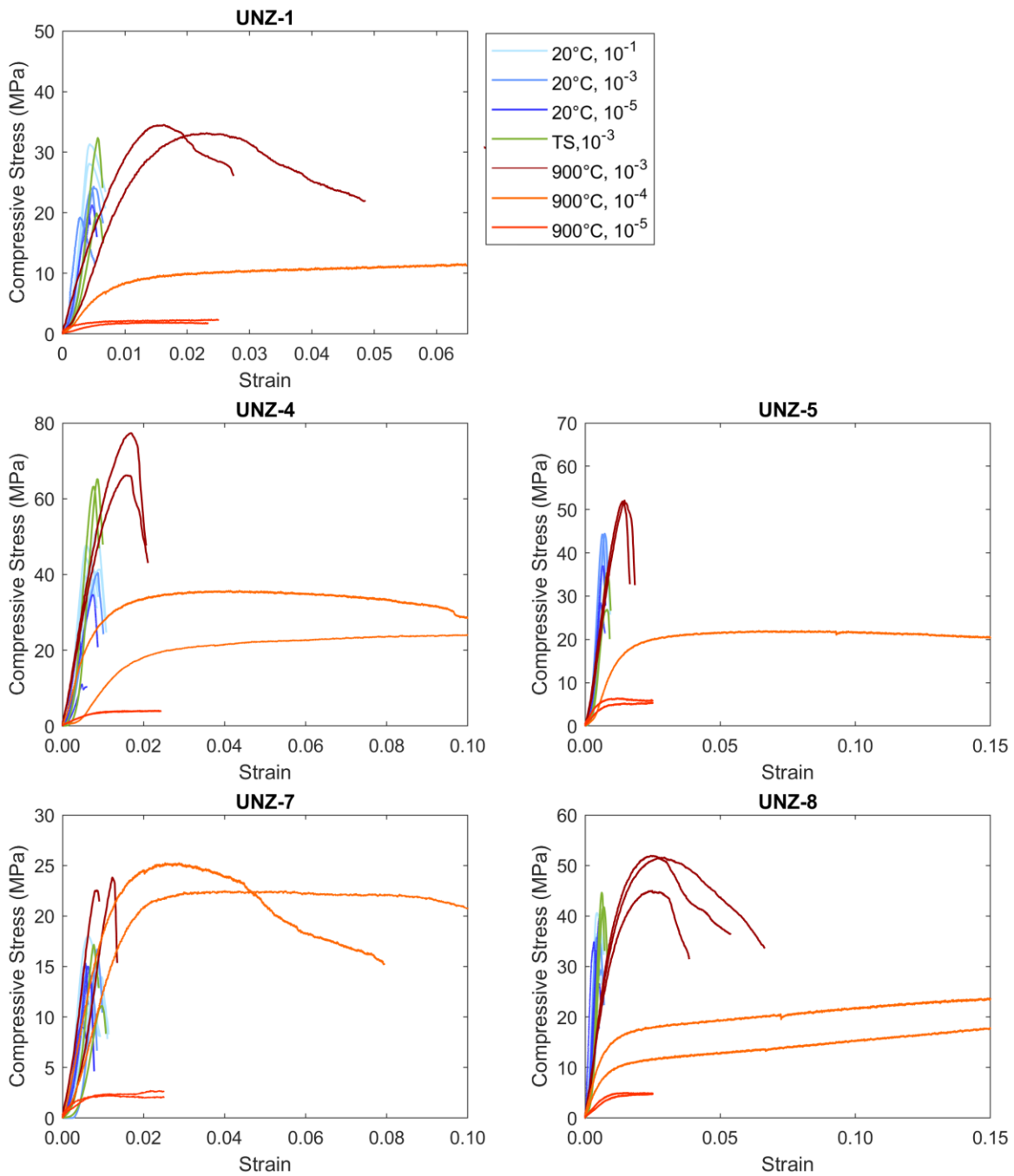
UNZ-13



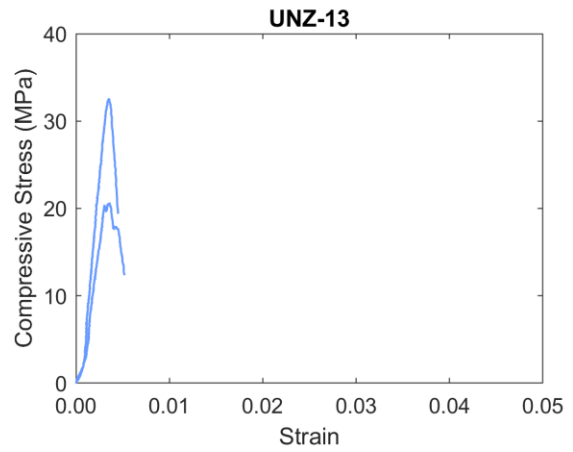
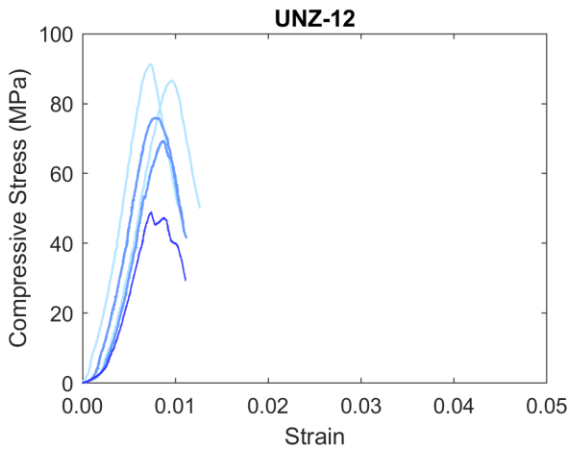
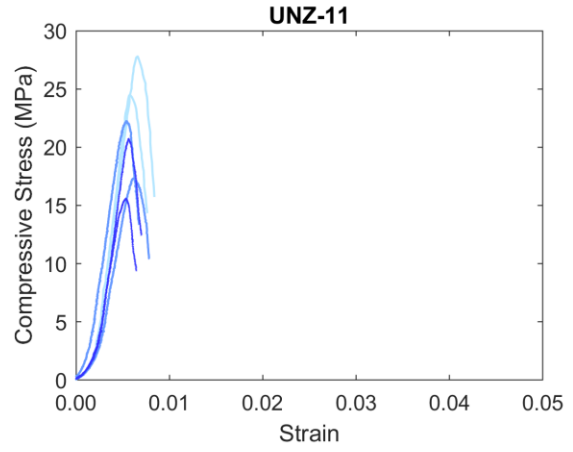
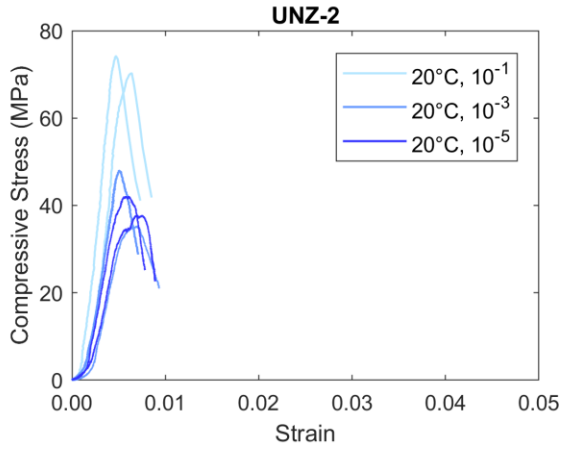
**S1. Images of cores used in the uniaxial compressive stress experiments. The principal stress,  $\sigma_1$ , was applied in the vertical direction. In all cores large phenocrysts of plagioclase and amphibole are recognisable, as well as a network of large pores and cracks. Signs of alteration are visible in certain cores, in UNZ-11 there is a crusty white/yellowish layer around pores and overall it has a friable texture, and in UNZ-12 a reddish hue is visible.**



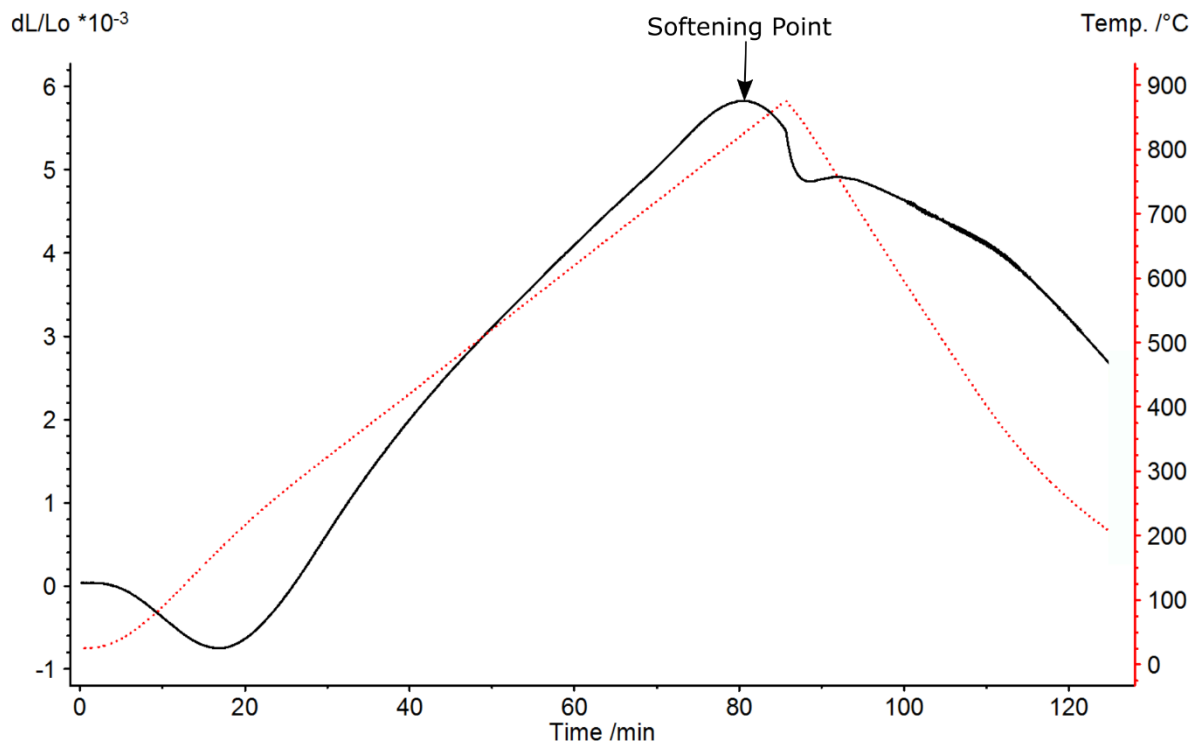
**S2. Backscattered electron images of all samples used in this study. These images were taken from polished stubs and are orientated so that the later applied principal stress,  $\sigma_1$ , was directed into the page.**



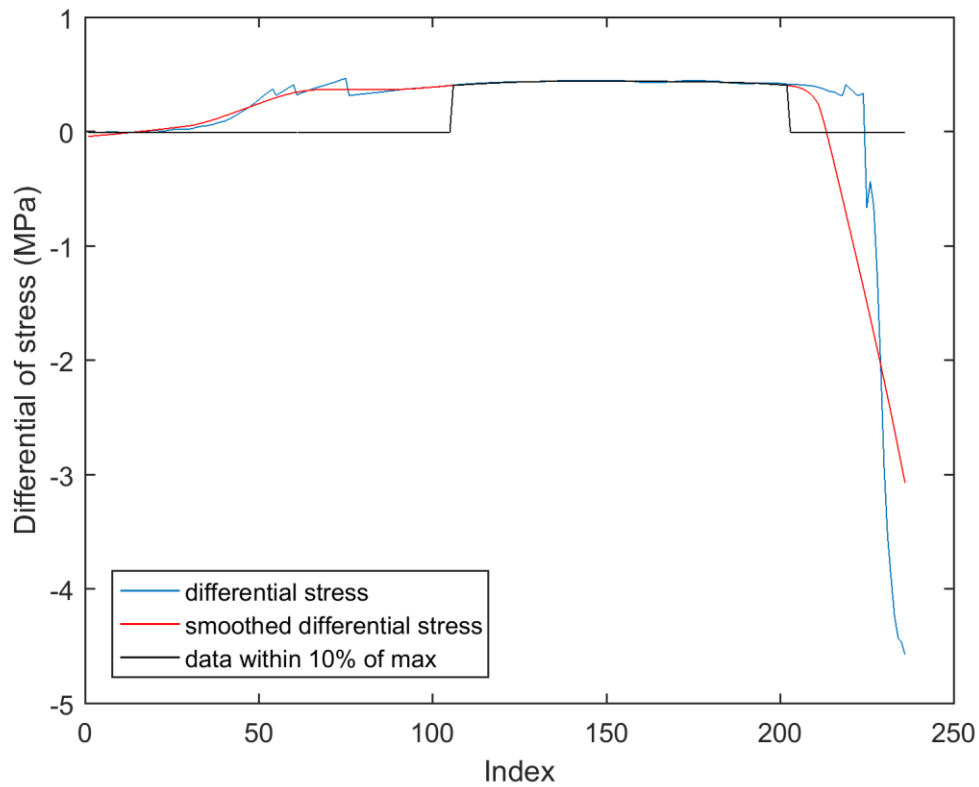
**S3. Stress-strain curves for uniaxial compressive strength tests conducted on thermally stressed and pristine samples at strain rates of  $10^{-1}$ ,  $10^{-3}$   $10^{-5} \text{ s}^{-1}$  at ambient temperatures, and on pristine samples at strain rates of  $10^{-3}$ ,  $10^{-4}$ ,  $10^{-5} \text{ s}^{-1}$  at temperatures of  $900^\circ\text{C}$ . The plots are separated into block number, and therefore porosity (see Table 3). These graphs show how strength is higher at both higher porosities and at higher temperatures. Thermally treated samples do not appear to vary in strength compared to their untreated equivalents, but do show a more concave-up initial portion of the curve. Experiments carried out at higher temperature and slower strain rates,  $10^{-4}$  and  $10^{-5} \text{ s}^{-1}$ , deform viscously in response to applied stress.**



**S4. Stress-strain curves for rocks deformed at strain rates of  $10^{-1}$ ,  $10^{-3}$  and  $10^{-5} \text{ s}^{-1}$  at ambient temperatures only. Here the curves demonstrate that samples deformed at higher strain rates achieve higher peak stresses across the range of porosities tested.**



**S5. Thermal analysis result showing the softening point of sample UNZ-8. The sample was heated at 10°C/min to 1100 °C whilst applying a constant load of 2N. The softening point was detected as 824.6 °C, 80.6 minutes into the experiment, when the applied load counteracted the thermal expansion of the sample, causing an inflection point (i.e. switch to contraction).**



**S6. Example plot (from sample UNZ-2-2) produced by the script run to find the Young's Modulus of a sample. The code looks at the gradient of the stress-strain curve and finds at which strains (the index number of the vector, x-axis) the increase in stress (y-axis) is at a maximum. The blue line shows the calculated differential of the stress, the red line is the differential stress smoothed, and the black line shows the points at which the stress is within 10 % of its maximum. The Young's modulus is then calculated with the resulting values of stress and strain from the black selector line, the maximum slope of the stress-strain curve.**